European Journal of Control 46 (2019) 80–89

Contents lists available at ScienceDirect

European Journal of Control

journal homepage: www.elsevier.com/locate/ejcon

# Analysis of consensus in hardware interconnected networks: An application to inverter-based AC microgrids

Miguel Parada Contzen*

*Electromechanics and Energy Conversion Department, Universidad de Talca, Chile*

ARTICLE INFO

*Article history:*
Received 8 May 2017
Revised 28 March 2018
Accepted 2 May 2018
Available online 9 May 2018

Recommended by G. Damm

*Keywords:*
Consensus
Distributed control
Linear matrix inequalities
AC microgrids

ABSTRACT

In this paper we address the problem of consensus in hardware interconnected networks. As an example of such, we focus on three-phase AC microgrids with Voltage Source Inverters (VSI) as generation units and the consensus control objectives of active power sharing and frequency synchronization. By distinguishing between the interconnected control plant, the control objectives, and the feedback controller, we analytically study a non-linear model of the power flow within the microgrid through a robust linear approximation. From here we suggest a Linear Matrix Inequality (LMI) based methodology to verify that the proposed control strategy makes the network reach the consensus objectives. The theoretical analysis is complemented with a simulation study of an arbitrary microgrid.



## 1. Introduction

Consensus is a topic that have been largely studied during the last decade. Most of the work in the area is based on Graph Theoretical approaches with single or double integrators dynamics for the agents and Laplacian consensus algorithms. Some examples are the books [16,23,24], or an increasing number of papers such as [1,5,8,9,17]. The particular dynamics with which these publications deal, makes it difficult to extend the results to other cases of interest. Although some publications deal with more general dynamical systems, e.g., [13,14,18,26,31,35,36], there are still many open questions. In particular, hardware interconnections become an interesting topic to address as it is difficult to assume that the controller design instance has the liberty to modify them. Furthermore, this becomes more intricate when the interconnections are non-linear in nature.

On another matter, microgrids are a promising solution for the integration of renewable power sources into the existing energy grid and for energy supply of remote areas. Some publications that deal with the general control of microgrids are [4,10,21,22,25]. In these systems the set of all generation units constitutes a network of agents that interact with each other through hardware interconnections, namely, through the electric grid. In this context, several publications deal with the problem of *power sharing* and *synchronization*, e.g., [11,19,20,27–30,32,33], two control objectives that can be addressed as consensus problems.

In this paper, we analytically study an arbitrary microgrid where all the generation units are assumed to be Voltage Source Inverters (VSI) as an example of a network of agents with hardware interconnections. These interconnections can be described by a trigonometric model what makes their analysis more challenging. The formal study of the system is done considering a classical control perspective, that is, identifying and modeling the microgrid itself as the control plant where control objectives are to be enforced by an appropriate controller. Based on existing strategies, we analyze a family of primary and secondary controllers to achieve respectively the control objectives of power sharing and synchronization. Even though some simplifications on the model of the plant are done, these are necessary to focus the discussion on the enforcement of the control objectives in the plant regardless of particular characteristics of the actuators, sensors, transmitters, or programmable controllers. The non-linear closed loop system is analyzed through a robust linear approximation in order to find sufficient conditions for both objectives in terms of Linear Matrix Inequalities (LMI).

The paper is organized as follows. Section 2 present some preliminary mathematical concepts concerning Graph Theory and (Moore-Penrose) pseudoinverses. Section 3 states the characteristics of the plant with which the paper deals. First the agents (the VSIs), as in several of the quoted publications, are modeled as simple integrators. The hardware interconnections between them are described through the non-linear model of the power injected by each inverter, what is explained in terms of the phase angles of

* Corresponding author.
*E-mail address:* miparada@utalca.cl

https://doi.org/10.1016/j.ejcon.2018.05.001

the induced voltages. This model is equivalently represented afterwards through the angle differences between nodes at each electric line of the grid. Next, a robust formulation for the analysis of non-linearities is presented considering a linear approximation of the model at the operation point. In Section 4, the closed loop system is formally analyzed. First the definitions of the control objectives (active power sharing and synchronization) are given as consensus problems. A primary droop-Laplacian controller for power sharing and a secondary distributed controller to achieve synchronization at nominal frequency are then proposed. From a closed loop analysis, sufficient conditions for power sharing and synchronization at nominal frequency in form of LMI tests are obtained. Section 5 presents some simulation examples to corroborate the discussed aspects.

Through this paper, matrix inequalities such as $\mathbf{A} < 0 (\mathbf{A} > 0)$ are used to indicate that matrix $\mathbf{A}$ is symmetric negative (or positive) definite. Matrix $\mathbf{A}'$ is the transpose of $\mathbf{A}$. The notation "$\star$" is used to indicate a symmetric block within a matrix. The identity matrix and the null matrix are respectively denoted by $\mathbf{I}$ and $\mathbf{0}$. A column vector of ones is denoted as $\mathbf{1}$, and a vector with zeros in every position except in the $i$-th row where its value is one, is denoted as $\mathbf{s}_i \in \mathbb{R}^N$ so that $\sum_{i=1}^{N} \mathbf{s}_i = \mathbf{1}$. If necessary, the dimensions of these matrices will be stated as an index. A (block) element in position $(i, j)$ of a matrix $\mathbf{A}$ is denoted $[\mathbf{A}]_{ij}$.

## 2. Preliminaries

### 2.1. Graph theory concepts

A graph $\mathcal{G} = (\mathcal{V}, \mathcal{E})$ is a set of nodes $\mathcal{V}$ and edges $\mathcal{E} \subseteq \mathcal{V} \times \mathcal{V}$. For further details refer to [7] or [16]. In the context of this work, the set of nodes (also called vertices) $\mathcal{V} = \{v_1, v_2, \ldots, v_N\}$ corresponds to controllable voltage sources and the existence of an edge $e_k = (v_i, v_j) \in \mathcal{E}$ means that node $i$ and node $j$ interact with each other in the sense of the input of node $j$ being the output of node $i$, or vice versa.

In an undirected graph, the edges are not ordered. We interpret the ordered pair $(v_i, v_j) \in \mathcal{E}$ as an undirected edge, that is, we ignore the implicit order of the pair. Hence we can write $(v_i, v_j) \iff (v_j, v_i) \in \mathcal{E}$, where $v_j \neq v_i$ ($(v_i, v_i) \notin \mathcal{E}$). The neighbor set of a node $i$ in an undirected graph $\mathcal{G}$ is defined as $\mathcal{N}_i = \{v_j \in \mathcal{V} | (v_i, v_j) \in \mathcal{E} \ \wedge \ i \neq j\}$. An undirected graph is connected if there is a path between every two nodes and unconnected otherwise. Any connected graph has at least $N-1$ edges. A (spanning) tree, denoted $\mathcal{T}$, is an undirected graph which is connected and has $N-1$ edges, where $N$ is the number of nodes.

A weighted graph $\mathcal{G}_w = (\mathcal{V}, \mathcal{E}, w)$ is a generalization of a graph and associates a weight to each edge through the function $w: \mathcal{E} \to \mathbb{R}^+$. The *Laplacian matrix* of an undirected weighted graph $\mathcal{G}_w$ is defined as $\hat{L}(\mathcal{G}_w) = \Delta(\mathcal{G}_w) - A(\mathcal{G}_w)$, where $A(\mathcal{G}_w) = [a_{ij}]$ is constructed so that $a_{ij} = w((v_i, v_j))$ if $(v_i, v_j) \in \mathcal{E}$ and 0 otherwise; $\Delta(\mathcal{G}_w) = diag\{d(v_1), \ldots, d(v_N)\}$; and $d(v_i) = \sum_j a_{ij} = \sum_i a_{ij}$. Then, each row and column of $\hat{L}(\mathcal{G}_w)$ sums up to zero. i.e., $\hat{L}(\mathcal{G}_w)\mathbf{1}_N = \mathbf{0}_{N\times 1}$ and $\mathbf{1}_N'\hat{L}(\mathcal{G}_w) = \mathbf{0}_{1\times N}$. It is a well known fact that $\hat{L}(\mathcal{G}_w)$ is positive semi-definite.

Strictly directed graphs, or strict digraphs, are graphs where each edge has an orientation. That is, we do not ignore the order of the pair $(v_i, v_j) \in \mathcal{E}$. Hence we can write, $(v_i, v_j) \in \mathcal{E} \Rightarrow (v_j, v_i) \notin \mathcal{E}$. For every undirected graph without self-loops, $2^{|\mathcal{E}|}$ strict digraphs can be defined by giving an orientation to every edge. An arbitrary strict digraph generated from an undirected graph $\mathcal{G}$ will be denoted by $\mathcal{G}^o$. The *Incidence Matrix*, denoted $D(\mathcal{G}^o)$, of such a strict digraph is defined as an $N \times |\mathcal{E}|$ matrix where each entry $o_{ik} = [D(\mathcal{G}^o)]_{ik}$ takes either the value $-1$ if the edge $e_k$ has its origin in $v_i$, $o_{ik} = 1$ if node $v_i$ is the destination of edge $e_k$ or $o_{ik} = 0$ otherwise. It can be shown that for an undirected weighted graph $\mathcal{G}_w = (\mathcal{G}, w)$, $\hat{L}(\mathcal{G}_w) = D(\mathcal{G}^o)\mathbf{W}D'(\mathcal{G}^o)$ where $\mathbf{W} = \text{diag}\left\{w((v_{i_k}, v_{j_k}))\right\}_{k=1}^{|\mathcal{E}|}$. Furthermore, if $\mathcal{G}$ is connected, then $\text{rank}\{D(\mathcal{G}^o)\} = \text{rank}\left\{\hat{L}(\mathcal{G}_w)\right\} = N-1$.

### 2.2. Some pseudoinverse properties

Given a matrix $\mathbf{A} \in \mathbb{C}^{m\times n}$, its unique *(Moore-Penrose) pseudoinverse*, $\mathbf{A}^+ \in \mathbb{C}^{n\times m}$, satisfies the *Penrose equations*:

$$\begin{aligned}
\mathbf{A}\mathbf{A}^+\mathbf{A} &= \mathbf{A},\\
\mathbf{A}^+\mathbf{A}\mathbf{A}^+ &= \mathbf{A}^+,\\
(\mathbf{A}\mathbf{A}^+)^* &= \mathbf{A}\mathbf{A}^+,\\
(\mathbf{A}^+\mathbf{A})^* &= \mathbf{A}^+\mathbf{A}.
\end{aligned}$$

where $\mathbf{A}^*$ is the conjugate transpose of $\mathbf{A}$. For more details the reader is referred to [3] or any other general reference.

For a matrix $\mathbf{A} \in \mathbb{C}^{m\times n}$, with $r = rank\{\mathbf{A}\} \leq \min\{m, n\}$, there are $\min\{m, n\}$ singular values, from which $r$ are nonzero. The singular values are usually labeled in descending order. The non-zero singular values of $\mathbf{A}$ are calculated as the square root of the eigenvalues of matrix $\mathbf{A}\mathbf{A}^*$: $\{\sigma > 0 | \sigma^2 \in \text{eig}\{\mathbf{A}\mathbf{A}^*\}\} \subseteq \text{svd}\{\mathbf{A}\}$.

The singular Values Decomposition (SVD), e.g., [3, Ch. 6.2], of a matrix $\mathbf{A} \in \mathbb{C}^{m\times n}$ with $r = rank\{\mathbf{A}\} > 0$ is such that $\mathbf{A} = \mathbf{U}\Sigma\mathbf{V}^*$, where

$$\Sigma = \mathbf{U}^*\mathbf{A}\mathbf{V} = \begin{bmatrix} \text{diag}\{\sigma_i\}_{i=1}^{r} & \mathbf{0}_{r\times(n-r)} \\ \mathbf{0}_{(m-r)\times r} & \mathbf{0}_{(m-r)\times(n-r)} \end{bmatrix} \in \mathbb{R}^{m\times n},$$

$\mathbf{U} = \text{row}\{\mathbf{u}_i\}_{i=1}^{m} \in \mathbb{C}^{m\times m}$, and $\mathbf{V} = \text{row}\{\mathbf{v}_i\}_{i=1}^{n} \in \mathbb{C}^{n\times n}$ are unitary matrices (i.e., $\mathbf{U}\mathbf{U}^* = \mathbf{U}^*\mathbf{U} = \mathbf{I}$ and $\mathbf{V}\mathbf{V}^* = \mathbf{V}^*\mathbf{V} = \mathbf{I}$), and $\mathbf{u}_i \in \mathbb{C}^m$ are the normalized eigenvectors of $\mathbf{A}\mathbf{A}^*$ and $\mathbf{v}_i \in \mathbb{C}^n$ the normalized eigenvectors of $\mathbf{A}^*\mathbf{A}$. Using the definition of pseudoinverse, it can be shown that

$$\mathbf{A}^+ = \mathbf{V}\Sigma^+\mathbf{U}^*,$$

where,

$$\Sigma^+ = \begin{bmatrix} \text{diag}\{1/\sigma_i\}_{i=1}^{r} & \mathbf{0}_{r\times(m-r)} \\ \mathbf{0}_{(n-r)\times r} & \mathbf{0}_{(n-r)\times(m-r)} \end{bmatrix} \in \mathbb{R}^{n\times m}.$$

If we decompose matrix $\mathbf{V} = \text{row}\{\mathbf{V}_+, \mathbf{V}_z\}$, where $\mathbf{V}_z = \text{row}\{\mathbf{v}_i\}_{i=r+1}^{n}$ (the eigenvectors associated to the zero eigenvalues of $\mathbf{A}^*\mathbf{A}$) and $\mathbf{V}_+ = \text{row}\{\mathbf{v}_i\}_{i=1}^{r}$, we found that

$$\begin{aligned}
\mathbf{A}^+\mathbf{A} &= \mathbf{V}\Sigma^+\mathbf{U}^*\mathbf{U}\Sigma\mathbf{V}^* = \mathbf{V}\Sigma\,\Sigma^+\mathbf{V}^*\\
&= \mathbf{V}\begin{bmatrix} \mathbf{I}_{r\times r} & \mathbf{0}_{r\times(n-r)} \\ \mathbf{0}_{(n-r)\times r} & \mathbf{0}_{(n-r)\times(n-r)} \end{bmatrix}\mathbf{V}^*\\
&= \mathbf{V}\left(\mathbf{I}_{n\times n} - \begin{bmatrix} \mathbf{0}_{r\times(n-r)} \\ \mathbf{I}_{(n-r)\times(n-r)} \end{bmatrix}\begin{bmatrix} \mathbf{0}_{(n-r)\times r} & \mathbf{I}_{(n-r)\times(n-r)} \end{bmatrix}\right)\mathbf{V}^*\\
&= \mathbf{I} - \begin{bmatrix} \mathbf{V}_+ & \mathbf{V}_z \end{bmatrix}\begin{bmatrix} \mathbf{0}_{r\times(n-r)} \\ \mathbf{I}_{(n-r)\times(n-r)} \end{bmatrix}\begin{bmatrix} \mathbf{0}_{(n-r)\times r} & \mathbf{I}_{(n-r)\times(n-r)} \end{bmatrix}\begin{bmatrix} \mathbf{V}_+^* \\ \mathbf{V}_z^* \end{bmatrix}\\
&= \mathbf{I} - \mathbf{V}_z\mathbf{V}_z^*.
\end{aligned}$$

Now consider a connected undirected graph $\mathcal{C} = (\mathcal{V}, \mathcal{E})$. We can define the matrix $\mathbf{D} = D'(\mathcal{C}^o) \in \mathbb{R}^{|\mathcal{E}|\times N}$, from any strict digraph $\mathcal{C}^o$ derived from $\mathcal{C}$. As $\text{rank}\{\mathbf{D}\} = N-1$ and $\mathbf{D}\mathbf{1} = \mathbf{0}$, we have that that the null space of $\mathbf{D}'\mathbf{D}$ is generated by the normalized vector $\mathbf{V}_z = \mathbf{D}^\perp = \frac{1}{\sqrt{N}}\mathbf{1}$. Therefore we have that,

$$\mathbf{D}^+\mathbf{D} = \mathbf{I} - \frac{1}{N}\mathbf{1}\mathbf{1}'. \tag{1}$$

In particular, for a tree $\mathcal{T} = (\mathcal{V}, \mathcal{E}_T)$, $\mathbf{T}^+\mathbf{T} = \mathbf{I} - \frac{1}{N}\mathbf{1}\mathbf{1}' \in \mathbb{R}^{N\times N}$ where $\mathbf{T} = D'(\mathcal{T}^o) \in \mathbb{R}^{(N-1)\times N}$.

Similarly, if we define the weighted undirected graph $\mathcal{C}_w = (\mathcal{C}, w)$, then matrix $\mathbf{C} = \hat{L}(\mathcal{C}_w) = \mathbf{D}'\mathbf{W}\mathbf{D}$, with $\mathbf{W} =$

$\text{diag}\{w((v_{i_k}, v_{j_k}))\}_{k=1}^{|\mathscr{E}|}$, also has the property

$$\mathbf{C}^{+}\mathbf{C} = \mathbf{I} - \frac{1}{N}\mathbf{1}\mathbf{1}'. \tag{2}$$

For simplicity, in the following we define matrix $\mathbf{J} = \frac{1}{N}\mathbf{1}\mathbf{1}'$. Note that for any weighted graph $\mathscr{G}_w$ we have that $\hat{L}(\mathscr{G}_w)\mathbf{J} = \mathbf{0}$.

## 3. Hardware interconnected network

### 3.1. Model and control of a voltage source inverter (VSI)

The model proposed in this section is based on the internal control strategies described in, e.g., [21,25]. The three-phase voltage output of a Voltage Source Inverter (VSI) can be described by its amplitude $V_i(t) > 0$ and its electric angle $\psi_i(t) := \omega t + \delta_i(t)$, where $\omega = 2\pi f > 0$ is a constant nominal angular frequency, with $f > 0$ the nominal frequency in Hertz, and $\delta_i(t) \in \mathbb{R}$ the phase shift angle with respect to an arbitrary reference.

At this control level, the intern dynamics of the inverters are typically neglected so that the input/output relation of the voltage operation (angular) frequency $\omega_{o,i} := \dot{\psi}_i(t)$ at node $i \in \mathscr{V}$, considering internal control loops, switching modulation and appropriate filtering, can be modeled as in [[27,29,30], etc.] with the following equation:

$$\dot{\psi}_i(t) = u^{\psi_i}(t),$$

where $u^{\psi_i}(t)$ is a frequency control input. This model assumes that each inverter is equipped with some DC storage unit, large enough to increase and decrease the AC power output in a certain range.

The inverter is operated around the nominal frequency $\omega$ and therefore its input is modified by:

$$u^{\psi_i}(t) = \omega + \kappa u_i(t),$$

where $u_i(t)$ is a control input and $\kappa > 0$ is a constant thought to limit the magnitude of signal $u_i$ after feedback.

With this, the intern dynamics of inverter $i$ can be written as a single integrator:

$$\dot{\delta}_i(t) = \kappa u_i(t). \tag{3}$$

The aggregation of all inverters corresponds to an integrator network typical to consensus problems. Nevertheless, these agents are interconnected by hardware relationships which are non-linear in nature, namely by the electrical grid. These interconnections, although one can model them through graph theoretical concepts, are part of the control plant over which a consensus problem can be defined.

Additionally, we are interested on the frequency deviation with respect to nominal frequency $\upsilon_i(t) := \dot{\psi}_i(t) - \omega = \dot{\delta}_i(t)$. Deriving Eq. (3), we can model the dynamics of the frequency deviation by the following expression

$$\dot{\upsilon}_i(t) = \kappa \dot{u}_i(t). \tag{4}$$

Frequency measurement is often costly, both computationally and economically. Therefore, we assume that $\upsilon_i(t)$ cannot be used for feedback.

From here, a microgrid can be characterized as a network of integrator agents by the following compact equation:

$$\boldsymbol{\upsilon} := \dot{\boldsymbol{\delta}} = \kappa \mathbf{u},$$

where $\boldsymbol{\delta} = \text{col}\{\delta_i(t)\}_{i\in\mathscr{V}}$ and $\mathbf{u} := \text{col}\{u_i(t)\}_{i\in\mathscr{V}}$. Note that $\dot{\boldsymbol{\upsilon}} = \kappa\dot{\mathbf{u}}$. This model does not include the effect of the electric grid on the inverters. That is, the hardware interconnections between the agents are not considered.

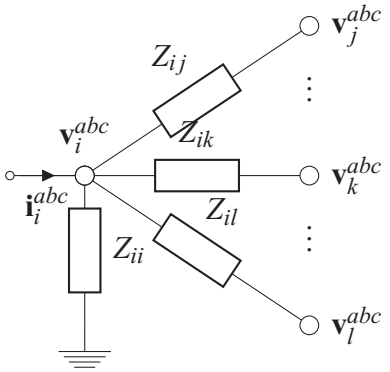


**Fig. 1.** Voltage and current at node $i$ of a microgrid with $\mathscr{N}_i = \{j, \ldots, k, \ldots, l\}$.

### 3.2. The electric grid as hardware interconnections

An electric grid can be described as an undirected graph $\mathscr{G} = (\mathscr{V}, \mathscr{E})$, where the vertices are a collection of $N$ electric nodes $i \in \mathscr{V}$ where three-phase generation units are connected, the undirected edges are transmission lines between the nodes, denoted $(i, j) \in \mathscr{E}$, and electric passive loads are present at every node. Any electric circuit can be equivalently represented by this structure through a Kron reduction procedure as described in [6]. It is also assumed that the grid is connected.

At every active node $i \in \mathscr{V}$, we will consider a balanced load described by time variant impedances composed by a resistance $R_{ii}$ in series with an inductance $L_{ii}$. A transmission line $(i, j) \in \mathscr{E}$ between nodes $i$ and $j \neq i$ will also be assumed as a balanced impedance composed by a resistance $R_{ij}$ in series with an inductance $L_{ij}$. Note that always $R_{ij} = R_{ji}$ and $L_{ij} = L_{ji}$. It is assumed that these line parameters are constant and can be estimated with reasonable accuracy.

When $\psi_i(t) = \omega t + \delta_i(t)$, a three phase balanced signal $\mathbf{x}^{abc}$ can be represented in an equivalent rotatory reference frame as $\mathbf{x}^{dq} = [\mathbf{x}^d, \mathbf{x}^q]'$ by means of Park's transformation [2,12]. In this notation, if $\mathbf{i}_i^{abc}$ is the current injected by an inverter in an active node $i$ and $\mathbf{v}_i^{abc}$ the voltage at that node, then the active power injected by the inverter can be defined by $P_i = \mathbf{i}_i^d\mathbf{v}_i^d + \mathbf{i}_i^q\mathbf{v}_i^q$. A dynamical relationship as function of the node voltages for the current can be obtained from a circuital analysis of the grid. A graphical representation of this can be seen in Fig. 1. If the transient behavior of the line dynamics is neglected, the active power flow can be simplified to

$$\begin{aligned} P_i(t) = {} & \frac{3}{2}\left[\frac{R_{ii}}{R_{ii}^2 + \omega^2 L_{ii}^2} + \sum_{j\in\mathscr{N}_i}\frac{R_{ij}}{R_{ij}^2 + \omega^2 L_{ij}^2}\right]V_i^2(t) + \ldots \\ & - \frac{3}{2}\sum_{j\in\mathscr{N}_i}\frac{R_{ij}}{R_{ij}^2 + \omega^2 L_{ij}^2}V_i(t)V_j(t)\cos\left(\delta_i(t) - \delta_j(t)\right) + \ldots \\ & + \frac{3}{2}\sum_{j\in\mathscr{N}_i}\frac{\omega L_{ij}}{R_{ij}^2 + \omega^2 L_{ij}^2}V_i(t)V_j(t)\sin\left(\delta_i(t) - \delta_j(t)\right) \end{aligned} \tag{5}$$

Where $\forall i \in \mathscr{V}$, $V_i(t)$ is the voltage amplitude at generation unit $i$ and $\delta_i(t)$ the corresponding phase angle. For simplicity, from here on we will drop the explicit time dependence of the variables. Note that the operation frequency at the $i$-th inverter, $\omega_{o,i} := \dot{\psi}_i = \omega + \dot{\delta}_i$, is not necessarily equal to the nominal value.

Instead of dealing directly with the injected power $P_i$ at node $i \in \mathscr{V}$ measured in $[kW]$ or $[MW]$, it is usual to treat power as a dimensionless quantity $\bar{P}_i$ measured in per unit $[p.u.]$. That is, relative to a base quantity $\chi_i > 0$, so that $\bar{P}_i = P_i/\chi_i$. A practical choice of the proportional constants would be the nominal power rating $S_i$ of the respective generation unit.

### 3.3. Non-linear hardware interconnections model

From Eq. (5), with constant voltage amplitudes ($V_i = V,\ \forall i \in \mathscr{V}$) we can write a non linear model for the power as

$$\mathbf{y} = \mathbf{c}(\boldsymbol{\delta}) + \mathbf{d}, \tag{6}$$

where,

$$\boldsymbol{\delta} = \text{col}\{\delta_i\}_{i\in\mathscr{V}},\ \ \mathbf{d} = \text{col}\{P_{ii}\}_{i\in\mathscr{V}},\ \ \mathbf{y} = \text{col}\{P_i\}_{i\in\mathscr{V}},$$

and $\mathbf{c}(\boldsymbol{\delta}) \in \mathbb{R}^N$ is a vector that depends on a nonlinear way of $\boldsymbol{\delta}$:

$$\mathbf{c}(\boldsymbol{\delta}) := \sum_{i\in\mathscr{V}} \mathbf{s}_i \sum_{j\in\mathscr{N}_i} \left(P_{ij}(1-\cos(\delta_i-\delta_j)) + Q_{ij}\sin(\delta_i-\delta_j)\right) \tag{7}$$

with

$$P_{ii}=\frac{3}{2}\frac{R_{ii}}{R_{ii}^2+\omega^2L_{ii}^2}V^2,\ \ P_{ij}=\frac{3}{2}\frac{R_{ij}}{R_{ij}^2+\omega^2L_{ij}^2}V^2,\ \ Q_{ij}=\frac{3}{2}\frac{\omega L_{ij}}{R_{ij}^2+\omega^2L_{ij}^2}V^2.$$

The assumption that the voltage amplitudes at every node are equal and constant, is done merely to simplify the following analysis. Dropping this assumption would lead to similar expressions, but would make the analysis more laborious, however without changing the general conclusions.

Note that the Jacobian matrix of (7) with respect to $\boldsymbol{\delta}$ can be written as a $\nabla_{\boldsymbol{\delta}}\mathbf{c} \in \mathbb{R}^{N\times N}$, that we will address as *flux matrix*, whose elements are given by

$$[\nabla_{\boldsymbol{\delta}}\mathbf{c}]_{ij} := \frac{\partial[\mathbf{c}(\boldsymbol{\delta})]_i}{\partial\delta_j}$$
$$= \begin{cases} \sum_{k\in\mathscr{N}_i} P_{ik}\sin(\delta_i-\delta_k) + Q_{ik}\cos(\delta_i-\delta_k) & \text{if } i=j, \\ -P_{ij}\sin(\delta_i-\delta_j) - Q_{ij}\cos(\delta_i-\delta_j) & \text{if } j\in\mathscr{N}_i, \\ 0 & \text{i.o.c.} \end{cases}$$

From this expression we have that the flux matrix has the zero row sum property: $(\nabla_{\boldsymbol{\delta}}\mathbf{c})\mathbf{1} = \mathbf{0}_{N\times 1}$. Observe further that

$$\frac{d}{dt}\mathbf{c}(\boldsymbol{\delta}) = (\nabla_{\boldsymbol{\delta}}\mathbf{c})\dot{\boldsymbol{\delta}}.$$

If we define a matrix

$$\mathbf{F} := \text{diag}\{1/\chi_i\}_{i\in\mathscr{V}},$$

then we have that $\bar{\mathbf{y}} := \mathbf{F}\mathbf{y} = \text{col}\{\bar{P}_i\}_{i\in\mathscr{V}}$ is the vector of the injected powers in per unit. Additionally, it is useful to define the per unit load $\bar{\mathbf{d}} = \mathbf{F}\mathbf{d}$ and the per unit load change rate $\bar{\mathbf{w}} = \mathbf{F}\dot{\mathbf{d}}$.

### 3.4. Hardware interconnections linear approximation

From Eq. (5), a simplified linear model can be obtained when $\delta_i(t) \approx \delta_j(t)$, so that $\sin(\delta_i-\delta_j) \approx \delta_i-\delta_j$ and $\cos(\delta_i-\delta_j) \approx 1$:

$$\mathbf{y} = \mathbf{C}\boldsymbol{\delta} + \mathbf{d}, \tag{8}$$

where matrix $\mathbf{C} \in \mathbb{R}^{N\times N}$ such that its elements are given $\forall i,j \in \{1,2,\ldots,N\}$ by:

$$[\mathbf{C}]_{ij} = \begin{cases} \sum_{k\in\mathscr{N}_i} Q_{ik} & \text{if } i=j, \\ -Q_{ij} & \text{if } j\in\mathscr{N}_i, \\ 0 & \text{i.o.c.} \end{cases}$$

As $Q_{ij} = Q_{ji}$, $\mathbf{C}\mathbf{1} = \mathbf{0}$. This implies that $\mathbf{C}$ is rank deficient as one of its eigenvalues is identically zero. The trigonometric model (6) is clearly more difficult to treat that the affine approximation (8).

### 3.5. Line angles representation

The quantity $\delta_i$ corresponds to the phase angle of the voltage signal at node $i$. It is however possible to study the behavior of the grid in terms of the angle differences $\theta_k := \psi_{i_k} - \psi_{j_k} = \delta_{i_k} - \delta_{j_k}$ defined over the $k$-th line $(i_k, j_k) \in \mathscr{E}$. Implicitly, this definition also fixes orientations to the edges because the angle differences are arbitrarily done in one particular order ($\theta_k := \delta_{i_k} - \delta_{j_k}$ and not $\theta_k := \delta_{j_k} - \delta_{i_k}$).

This can be studied by defining matrix $\mathbf{D} = D'(\mathscr{C}^o) \in \mathbb{R}^{|\mathscr{E}|\times N}$, with $\mathscr{C} := (\mathscr{V}, \mathscr{E})$ the undirected graph representing the grid. Note that this is not unique as the strict digraph $\mathscr{C}^o$ is arbitrary. Furthermore, as the orientations of the edges are arbitrary, the matrix could be equivalently defined as $\mathbf{D} = -D'(\mathscr{C}^o)$, i.e., altering the order of the differences that define the line angles, without any change on the following development. By construction we have that $\mathbf{D}\mathbf{1} = \mathbf{0}$. As the multiplication $\boldsymbol{\theta} := \mathbf{D}\boldsymbol{\delta}$ computes the differences between the angles of two neighboring nodes, then $\boldsymbol{\theta} = \text{col}\{\theta_k\}_{k=1}^{|\mathscr{E}|}$.

With this, the linear model matrix $\mathbf{C}$ can be rewritten in terms of the lines between generation units, $(i_k, j_k) \in \mathscr{E}$:

$$\mathbf{C} = \mathbf{D}'\mathbf{W}\mathbf{D} = \sum_{k=1}^{|\mathscr{E}|} \left(\mathbf{s}_{i_k} - \mathbf{s}_{j_k}\right) Q_{i_kj_k} \left(\mathbf{s}_{i_k} - \mathbf{s}_{j_k}\right)', \tag{9}$$

where $\mathbf{W} = \text{diag}\left\{Q_{i_kj_k}\right\}_{k=1}^{|\mathscr{E}|}$.

The non-linear expression (7) can also be written in terms of the lines between generation units, $(i_k, j_k) \in \mathscr{E}$, as

$$\mathbf{c}(\boldsymbol{\delta})\Big|_{\boldsymbol{\theta}=\mathbf{D}\boldsymbol{\delta}} = \sum_{k=1}^{|\mathscr{E}|} \Big[ \left(\mathbf{s}_{i_k} + \mathbf{s}_{j_k}\right) P_{i_kj_k}(1-\cos(\theta_k)) + \left(\mathbf{s}_{i_k} - \mathbf{s}_{j_k}\right) Q_{i_kj_k}\sin(\theta_k) \Big],$$

with $\boldsymbol{\theta} = \mathbf{D}\boldsymbol{\delta}$. In this case, the flux matrix can be evaluated at the angle differences and written as

$$\nabla_{\boldsymbol{\delta}}\mathbf{c} = \sum_{k=1}^{|\mathscr{E}|} \Big[ \left(\mathbf{s}_{i_k} + \mathbf{s}_{j_k}\right) P_{i_kj_k}\sin(\theta_k) \left(\mathbf{s}_{i_k} - \mathbf{s}_{j_k}\right)' + \left(\mathbf{s}_{i_k} - \mathbf{s}_{j_k}\right) Q_{i_kj_k}\cos(\theta_k) \left(\mathbf{s}_{i_k} - \mathbf{s}_{j_k}\right)' \Big]. \tag{10}$$

Note that the flux matrix is the gradient of $\mathbf{c}(\boldsymbol{\delta})$ with respect to $\boldsymbol{\delta}$, which is not the same as the gradient of $\mathbf{c}(\boldsymbol{\delta})$ with respect to $\boldsymbol{\theta}$. Indeed, the last one is

$$\nabla_{\boldsymbol{\theta}}\mathbf{c} = \sum_{k=1}^{|\mathscr{E}|} \Big[ \left(\mathbf{s}_{i_k} + \mathbf{s}_{j_k}\right) P_{i_kj_k}\sin(\theta_k) + \left(\mathbf{s}_{i_k} - \mathbf{s}_{j_k}\right) Q_{i_kj_k}\cos(\theta_k) \Big] \hat{\mathbf{s}}_k' \in \mathbb{R}^{N\times|\mathscr{E}|},$$

where $[\nabla_{\boldsymbol{\theta}}\mathbf{c}]_{ik} = \frac{\partial[\mathbf{c}(\boldsymbol{\delta})]_i}{\partial\theta_k}$, and $\hat{\mathbf{s}}_k \in \mathbb{R}^{|\mathscr{E}|}$ is a vector with zeros in every row except for the $k$-th row where the value is one. It is easy to verify that $\nabla_{\boldsymbol{\delta}}\mathbf{c} = (\nabla_{\boldsymbol{\theta}}\mathbf{c})\mathbf{D}$. Furthermore,

$$\nabla_{\boldsymbol{\theta}}\mathbf{c}|_{\boldsymbol{\theta}=\mathbf{0}} = \sum_{k=1}^{|\mathscr{E}|} \left(\mathbf{s}_{i_k} - \mathbf{s}_{j_k}\right) Q_{i_kj_k} \hat{\mathbf{s}}_k' = \mathbf{D}'\mathbf{W}.$$

Therefore, $\mathbf{D}'\mathbf{W}\boldsymbol{\theta} = \mathbf{D}'\mathbf{W}\mathbf{D}\boldsymbol{\delta} = \mathbf{C}\boldsymbol{\delta} \approx \mathbf{c}(\boldsymbol{\delta})\big|_{\boldsymbol{\theta}=\mathbf{D}\boldsymbol{\delta}}$ is a Tylor linear approximation around the operation point $\boldsymbol{\theta} = \mathbf{0}$ of the power flow in the grid. Lyapunov's linearization criterion leads then to conclude that any stability result derived from the linear representation of the system is sufficient to guarantee local stability around $\boldsymbol{\theta} \approx \mathbf{0}$. Therefore, they are also necessary conditions for global stability of the non-linear system.

### 3.6. A robust approximation of the non-linear model

When the angle differences over the lines are small, one can analyze the grid by its linear representation. The difference between this simplified model and the one including all non-linearities can be interpreted as parametric uncertainties for the linear model and addressed through a robustness approach. For this, consider that, $\forall k \in \{1, 2, \ldots, |\mathscr{E}|\}$, we known a value $0 < \epsilon_k < \pi/2$ such that $-\epsilon_k \leq \theta_k \leq \epsilon_k$. Then we have that

$$\begin{aligned} -\sin(\epsilon_k) \leq \sin(\theta_k) \leq \sin(\epsilon_k), \\ 0 < \cos(\epsilon_k) \leq \cos(\theta_k) \leq 1. \end{aligned} \tag{11}$$

Define matrices

$$\Delta \mathbf{C}_P(t) := \sum_{k=1}^{|\mathscr{E}|} \left(\mathbf{s}_{i_k} + \mathbf{s}_{j_k}\right) P_{i_k j_k} \Delta_{p,k}(t) \left(\mathbf{s}_{i_k} - \mathbf{s}_{j_k}\right)',$$

$$\Delta \mathbf{C}_Q(t) := \sum_{k=1}^{|\mathscr{E}|} \left(\mathbf{s}_{i_k} - \mathbf{s}_{j_k}\right) Q_{i_k j_k} \left( \Delta_{q,k}(t) - \frac{1-\cos(\epsilon_k)}{2} \right) \left(\mathbf{s}_{i_k} - \mathbf{s}_{j_k}\right)',$$

where $\forall (i_k, j_k) \in \mathscr{E}$, $\Delta_{p,k}(t) \in \mathbb{R}$ and $\Delta_{q,k}(t) \in \mathbb{R}$ are unknown quantities that compress all possible nonlinearities of the flux matrix. With this, we can enforce that

$$\begin{aligned} \nabla_{\boldsymbol{\delta}} \mathbf{c} &\stackrel{!}{=} \mathbf{C} + \Delta \mathbf{C}_P(t) + \Delta \mathbf{C}_Q(t) \\ &= \sum_{k=1}^{|\mathscr{E}|} \Big[ \left(\mathbf{s}_{i_k} + \mathbf{s}_{j_k}\right) P_{i_k j_k} \Delta_{p,k}(t) \left(\mathbf{s}_{i_k} - \mathbf{s}_{j_k}\right)' + \ldots \\ &\quad \ldots + \left(\mathbf{s}_{i_k} - \mathbf{s}_{j_k}\right) Q_{i_k j_k} \left( 1 + \Delta_{q,k}(t) - \frac{1-\cos(\epsilon_k)}{2} \right) \left(\mathbf{s}_{i_k} - \mathbf{s}_{j_k}\right)' \Big]. \end{aligned}$$

This expression can be interpreted as an uncertain linear approximation of the flux matrix decomposed with respect to the lines between generation units. Comparing this last expression with (10), it is sufficient for a robust analysis to impose that $\forall (i_k, j_k) \in \mathscr{E}$,

$$\Delta_{p,k}(t) \stackrel{!}{=} \sin(\theta_k),$$

and

$$1 + \Delta_{q,k}(t) - \frac{1-\cos(\epsilon_k)}{2} \stackrel{!}{=} \cos(\theta_k).$$

Considering the bounds in (11), the equality case is contained in the region described by

$$|\Delta_{p,k}(t)| \leq \sin(\epsilon_k), \tag{12}$$

$$|\Delta_{q,k}(t)| \leq \frac{1-\cos(\epsilon_k)}{2}. \tag{13}$$

This bounds can be used to analyze the grid by treating the non-linearities of matrix $\nabla_{\boldsymbol{\delta}} \mathbf{c}$ as bounded uncertain quantities described by $\Delta_{p,k}(t)$ and $\Delta_{q,k}(t)$. Of course, this procedure would lead to conservative criteria because part of the non-linear information is neglected. In particular, the Pythagorean relation between the trigonometric quantities is lost if only higher and lower bounds for $\Delta_{p,k}(t)$ and $\Delta_{q,k}(t)$ are considered. This can be seen in Fig. 2, where the blue shaded area corresponds to the robust area described by (11). Clearly, to impose a criterion to all the points in the area is more conservative that only imposing the criterion to the arc that describes exactly the nonlinearities.

## 4. Closed loop analysis

### 4.1. Control objectives

We are interested on a primary control objective known in the microgrid terminology as *power sharing*. This can be simply understood as that all the per unit power injected by each inverter

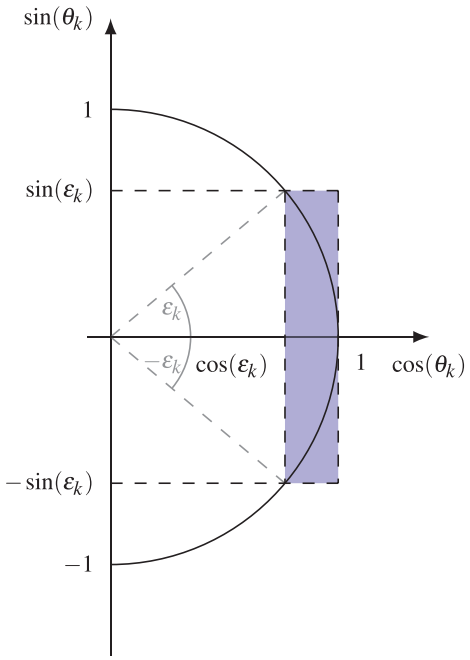


**Fig. 2.** Robust treatment of non-linearities.

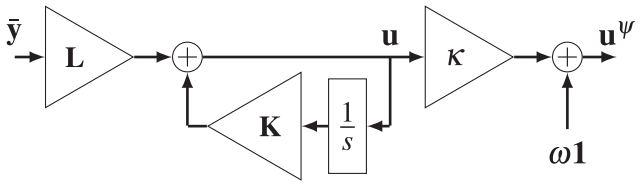


**Fig. 3.** Control strategy for a microgrid with only VSI as generation units.

$\bar{P}_i = [\bar{\mathbf{y}}]_i$ are equal in the long term. i.e., for all $i$ and $j \in \mathscr{V}$

$$\lim_{t \to +\infty} [\bar{\mathbf{y}}]_i = \lim_{t \to +\infty} [\bar{\mathbf{y}}]_j.$$

This is a consensus problem and can be studied through the following transformation as in [20]:

$$\mathbf{T} = \begin{bmatrix} \mathbf{1}_{N-1} & -\mathbf{I}_{N-1} \end{bmatrix} \in \mathbb{R}^{(N-1)\times N}.$$

In general, any transformation $\mathbf{T} = D'(\mathscr{T}^o)$ derived from an unweighted spanning directed tree $\mathscr{T}^o$ can be chosen. We define the previous one just for clarity. Each element of the vector

$$\mathbf{e}_y = \mathbf{T}\bar{\mathbf{y}} \tag{14}$$

is the difference of the normalized active power of the first generation unit with respect to the other generation units. Therefore if $\mathbf{e}_y$ asymptotically approaches the origin, the microgrid reaches power sharing.

The pseudoinverse of $\mathbf{T}$ can be calculated as $\mathbf{T}^+ = \mathbf{T}'(\mathbf{T}\mathbf{T}')^{-1}$. Note that because of (1), pre-multiplying Eq. (14) by $\mathbf{T}^+$ leads to

$$\bar{\mathbf{y}} = \mathbf{T}^+ \mathbf{e}_y + \mathbf{J}\bar{\mathbf{y}}. \tag{15}$$

As matrix $\mathbf{T}$ is a reduction of order, $\bar{\mathbf{y}} \in \mathbb{R}^N$ cannot be written as a function of $\mathbf{e}_y \in \mathbb{R}^{N-1}$ only.

Additionally, we are interested on a secondary control objective. It is desired that the operation frequency $\omega_{o,i} = \dot{\psi}_i = \omega + \upsilon_i$ at every node $i \in \mathscr{V}$ is the same. When this happens it is said that the generation units are *synchronized*. This is also a consensus problem and can be treated similarly as power sharing. Nevertheless, it is of further interest that synchronization is reached at the nominal

frequency $\omega$. This can be achieved by imposing that the frequency deviation vector,

$$\boldsymbol{\upsilon} := \text{col}\{\upsilon_i\}_{i\in\mathscr{V}} = \dot{\boldsymbol{\delta}}, \tag{16}$$

asymptotically approaches the origin.

### 4.2. Feedback controller

The following control law can be proposed:

$$\mathbf{u} = \mathbf{L}\bar{\mathbf{y}} + \mathbf{K}\int_0^t \mathbf{u}(\tau)d\tau, \tag{17}$$

where $\mathbf{L} = -l\mathbf{I} - \hat{L}(\mathscr{G}_w) \in \mathbb{R}^{N\times N}$ is the primary feedback matrix with $\mathscr{G}_w$ a given weighted undirected graph, and $l > 0$ a droop constant; and $\mathbf{K} \in \mathbb{R}^{N\times N}$ is a secondary feedback matrix given by

$$\mathbf{K} := -\mathbf{1}\mathbf{k}', \tag{18}$$

with $\mathbf{k} \in \mathbb{R}^N_{\geq 0}$ an arbitrary vector with nonnegative elements. The idea of using primary and secondary level controllers is well documented in the available references, for example [28,33], and several variations of the family of control strategies defined by (17) can be found. In particular, this is similar to the controller proposed in [11], which is a special case of (17).

A traditional droop controller refers to the special case where $\hat{L}(\mathscr{G}_w) = \mathbf{0}$ and $\mathbf{k} = \mathbf{0}$. As $\boldsymbol{\upsilon} := \dot{\boldsymbol{\delta}} = \kappa\mathbf{u}$, the secondary integral action can be interpreted as a frequency deviation integral feedback but with the advantage that frequency does not need to be directly measured.

In practice, the off diagonal elements of the feedback matrices imply that signals need to be communicated from one generation unit to another and therefore are avoided. However, in [19] it is shown that the exchange of signals between the generation units can improve the power sharing performance. On the other side, the exchange of signals at secondary control level is necessary for synchronization at nominal frequency. Note that if we choose $\mathbf{k} = k\mathbf{s}_i$, for some $i \in \mathscr{V}$ and $k > 0$, we only need to communicate the frequency information of the $i$-th node to the rest and only $N-1$ frequency signals need to be actively exchanged.

### 4.3. Non-linear closed loop behavior

Consider that the power flow in the microgrid is modeled by the non linear equation (6). From the studied controller (17), with known feedback gains $\mathbf{L} = -l\mathbf{I} - \hat{L}(\mathscr{G}_w)$ and $\mathbf{K} = -\mathbf{1}\mathbf{k}'$, we obtain from the definition of the error that

$$\begin{aligned}
\dot{\mathbf{e}}_y &= \mathbf{T}\mathbf{F}\dot{\mathbf{y}} \\
&= \mathbf{T}\mathbf{F}\frac{d}{dt}\mathbf{c}(\boldsymbol{\delta}) + \mathbf{T}\bar{\mathbf{w}} \\
&= \mathbf{T}\mathbf{F}(\nabla_{\boldsymbol{\delta}}\mathbf{c})\dot{\boldsymbol{\delta}} + \mathbf{T}\bar{\mathbf{w}} \\
&= \kappa\mathbf{T}\mathbf{F}(\nabla_{\boldsymbol{\delta}}\mathbf{c})\mathbf{u} + \mathbf{T}\bar{\mathbf{w}} \\
&= \kappa\mathbf{T}\mathbf{F}(\nabla_{\boldsymbol{\delta}}\mathbf{c})\left(\mathbf{L}\mathbf{T}^+\mathbf{e}_y + \mathbf{L}\mathbf{J}\bar{\mathbf{y}} + \mathbf{K}\int_0^t \mathbf{u}d\tau\right) + \mathbf{T}\bar{\mathbf{w}}.
\end{aligned}$$

With $\bar{\mathbf{w}} = \mathbf{F}\dot{\mathbf{d}}$. Because $(\nabla_{\boldsymbol{\delta}}\mathbf{c})\mathbf{1} = \mathbf{0}$, then

$$\dot{\mathbf{e}}_y = \kappa\mathbf{T}\mathbf{F}(\nabla_{\boldsymbol{\delta}}\mathbf{c})\mathbf{L}\mathbf{T}^+\mathbf{e}_y + \mathbf{T}\bar{\mathbf{w}}. \tag{19}$$

Furthermore, from (17) we have that

$$\begin{aligned}
\dot{\mathbf{u}} &= \mathbf{L}\mathbf{F}\dot{\mathbf{y}} + \mathbf{K}\mathbf{u} \\
&= \mathbf{L}\mathbf{F}\frac{d}{dt}\mathbf{c}(\boldsymbol{\delta}) + \mathbf{L}\bar{\mathbf{w}} + \mathbf{K}\mathbf{u} \\
&= \mathbf{L}\mathbf{F}(\nabla_{\boldsymbol{\delta}}\mathbf{c})\dot{\boldsymbol{\delta}} + \frac{1}{\kappa}\mathbf{K}\boldsymbol{\upsilon} + \mathbf{L}\bar{\mathbf{w}} \\
&= \left(\mathbf{L}\mathbf{F}(\nabla_{\boldsymbol{\delta}}\mathbf{c}) + \frac{1}{\kappa}\mathbf{K}\right)\boldsymbol{\upsilon} + \mathbf{L}\bar{\mathbf{w}}.
\end{aligned}$$

And then,

$$\dot{\boldsymbol{\upsilon}} = \kappa\dot{\mathbf{u}} = (\kappa\mathbf{L}\mathbf{F}(\nabla_{\boldsymbol{\delta}}\mathbf{c}) + \mathbf{K})\boldsymbol{\upsilon} + \kappa\mathbf{L}\bar{\mathbf{w}}. \tag{20}$$

Therefore, under constant load, i.e., when $\bar{\mathbf{w}} = \mathbf{0}$, power sharing and synchronization are achieved with the specified controller if the non linear systems (19) and (20) are asymptotically stable.

As noted before, locally in the vicinity of $\boldsymbol{\theta} = \mathbf{0}$, we have that $\nabla_{\boldsymbol{\delta}}\mathbf{c} \approx \mathbf{C}$. Therefore, necessary conditions for global power sharing and synchronization are that, respectively, the matrices $\mathbf{G}_y := \kappa\mathbf{T}\mathbf{F}\mathbf{C}\mathbf{L}\mathbf{T}^+$ and $\mathbf{G}_K := \kappa\mathbf{L}\mathbf{F}\mathbf{C} + \mathbf{K}$ are Hurwitz.

### 4.4. Robust approach to consensus in microgrids

To deal with the stability of the non-linear systems we can consider the general system

$$\dot{\mathbf{x}} = (\mathbf{A} + \mathbf{N}(\nabla_{\boldsymbol{\delta}}\mathbf{c})\mathbf{M})\mathbf{x}, \tag{21}$$

with matrices $\mathbf{A}$, $\mathbf{N}$, and $\mathbf{M}$ of proper dimensions. Clearly, systems (19) and (20) are special cases of (21) when the load is constant (when $\bar{\mathbf{w}} = \mathbf{0}$). It follows from the Lyapunov function $v = \mathbf{x}'\mathbf{P}\mathbf{x} > 0$, that a sufficient condition for stability of (21) is the existence of $\mathbf{P} = \mathbf{P}' > 0$ such that

$$\mathbf{P}\mathbf{A} + \mathbf{A}'\mathbf{P} + \mathbf{P}\mathbf{N}(\nabla_{\boldsymbol{\delta}}\mathbf{c})\mathbf{M} + \mathbf{M}'(\nabla_{\boldsymbol{\delta}}\mathbf{c})'\mathbf{N}'\mathbf{P} < 0. \tag{22}$$

Considering the robust linear approximation of the flux matrix, i.e., $\nabla_{\boldsymbol{\delta}}\mathbf{c} = \mathbf{C} + \Delta\mathbf{C}_P(t) + \Delta\mathbf{C}_Q(t)$, when $\forall k \in \{1, 2, \ldots, |\mathscr{E}|\}$, $|\theta_k| \leq \epsilon_k$, we can write

$$\begin{aligned}
&\mathbf{P}\mathbf{N}(\nabla_{\boldsymbol{\delta}}\mathbf{c})\mathbf{M} \\
&\quad= \mathbf{P}\mathbf{N}\mathbf{C}\mathbf{M} + \mathbf{P}\mathbf{N}\Delta\mathbf{C}_P(t)\mathbf{M} + \mathbf{P}\mathbf{N}\Delta\mathbf{C}_Q(t)\mathbf{M} \\
&\quad= \sum_{k=1}^{|\mathscr{E}|}\left[\mathbf{P}\mathbf{N}\left(\mathbf{s}_{i_k} - \mathbf{s}_{j_k}\right)Q_{i_kj_k}\left(\mathbf{s}_{i_k} - \mathbf{s}_{j_k}\right)'\mathbf{M}\right] + \ldots \\
&\qquad\ldots + \sum_{k=1}^{|\mathscr{E}|}\left[\mathbf{P}\mathbf{N}\left(\mathbf{s}_{i_k} + \mathbf{s}_{j_k}\right)P_{i_kj_k}\Delta_{p,k}(t)\left(\mathbf{s}_{i_k} - \mathbf{s}_{j_k}\right)'\mathbf{M}\right] + \ldots \\
&\qquad\ldots + \sum_{k=1}^{|\mathscr{E}|}\left[\mathbf{P}\mathbf{N}\left(\mathbf{s}_{i_k} - \mathbf{s}_{j_k}\right)Q_{i_kj_k}\left(\Delta_{q,k}(t) - \frac{1-\cos(\epsilon_k)}{2}\right)\right. \\
&\qquad\left.\times\left(\mathbf{s}_{i_k} - \mathbf{s}_{j_k}\right)'\mathbf{M}\right] \\
&\quad= \frac{1}{2}\sum_{k=1}^{|\mathscr{E}|}\left[\mathbf{P}\mathbf{N}\left(\mathbf{s}_{i_k} - \mathbf{s}_{j_k}\right)Q_{i_kj_k}(1+\cos(\epsilon_k))\left(\mathbf{s}_{i_k} - \mathbf{s}_{j_k}\right)'\mathbf{M}\right] + \ldots \\
&\qquad\ldots + \sum_{k=1}^{|\mathscr{E}|}\left[\mathbf{P}\mathbf{N}\left(\mathbf{s}_{i_k} + \mathbf{s}_{j_k}\right)P_{i_kj_k}\Delta_{p,k}(t)\left(\mathbf{s}_{i_k} - \mathbf{s}_{j_k}\right)'\mathbf{M}\right] + \ldots \\
&\qquad\ldots + \sum_{k=1}^{|\mathscr{E}|}\left[\mathbf{P}\mathbf{N}\left(\mathbf{s}_{i_k} - \mathbf{s}_{j_k}\right)Q_{i_kj_k}\Delta_{q,k}(t)\left(\mathbf{s}_{i_k} - \mathbf{s}_{j_k}\right)'\mathbf{M}\right].
\end{aligned} \tag{23}$$

Before proceeding, note that for any matrices $\mathbf{P} = \mathbf{P}'$, $\mathbf{X}_k$, and $\mathbf{Y}_k$ of proper dimensions, and scalars $\Delta_k > 0$, and $\mu_k > 0$ the following statement is always true:

$$\left(\frac{1}{\sqrt{\mu_k}}\mathbf{P}\mathbf{X}_k - \sqrt{\mu_k}\Delta_k\mathbf{Y}_k'\right)\left(\frac{1}{\sqrt{\mu_k}}\mathbf{P}\mathbf{X}_k - \sqrt{\mu_k}\Delta_k\mathbf{Y}_k'\right)' \geq 0.$$

Equivalently, by factorization of the previous expression,

$$\mathbf{P}\mathbf{X}_k\Delta_k\mathbf{Y}_k + \mathbf{Y}_k'\Delta_k\mathbf{X}_k'\mathbf{P} \leq \frac{1}{\mu_k}\mathbf{P}\mathbf{X}_k\mathbf{X}_k'\mathbf{P} + \mu_k\mathbf{Y}_k'\Delta_k^2\mathbf{Y}_k. \tag{24}$$

From expression (23), using property (24) over the terms associated to $\Delta_{p,k}(t)$ and $\Delta_{q,k}(t)$, that is, identifying the matrices

$$\mathbf{X}_{k,p} = \mathbf{N}\left(\mathbf{s}_{i_k} + \mathbf{s}_{j_k}\right)P_{i_k j_k}, \quad \mathbf{Y}_{k,p} = \left(\mathbf{s}_{i_k} - \mathbf{s}_{j_k}\right)'\mathbf{M},$$
$$\mathbf{X}_{k,q} = \mathbf{N}\left(\mathbf{s}_{i_k} - \mathbf{s}_{j_k}\right)Q_{i_k j_k}, \quad \mathbf{Y}_{k,q} = \left(\mathbf{s}_{i_k} - \mathbf{s}_{j_k}\right)'\mathbf{M},$$

an upper bound for the non-linear term at the left hand side of stability condition (22) can be found:

$$\begin{aligned}
&\mathbf{PN}(\nabla_{\boldsymbol{\delta}}\mathbf{c})\mathbf{M} + \mathbf{M}'(\nabla_{\boldsymbol{\delta}}\mathbf{c})'\mathbf{N}'\mathbf{P} \\
&\quad \le \mathbf{PNC}_\epsilon\mathbf{M} + \mathbf{M}'\mathbf{C}_\epsilon'\mathbf{N}'\mathbf{P} + \dots \\
&\quad \dots + \sum_{k=1}^{|\mathscr{E}|}\Bigg[\frac{1}{\mu_k}\mathbf{PN}\left(\mathbf{s}_{i_k} + \mathbf{s}_{j_k}\right)P_{i_k j_k}^2\left(\mathbf{s}_{i_k} + \mathbf{s}_{j_k}\right)'\mathbf{N}'\mathbf{P} + \dots \\
&\qquad \dots + \mu_k\mathbf{M}'\left(\mathbf{s}_{i_k} - \mathbf{s}_{j_k}\right)\Delta_{p,k}^2(t)\left(\mathbf{s}_{i_k} - \mathbf{s}_{j_k}\right)'\mathbf{M}\Bigg] + \dots \\
&\quad \dots + \sum_{k=1}^{|\mathscr{E}|}\Bigg[\frac{1}{\mu_k}\mathbf{PN}\left(\mathbf{s}_{i_k} - \mathbf{s}_{j_k}\right)Q_{i_k j_k}^2\left(\mathbf{s}_{i_k} - \mathbf{s}_{j_k}\right)'\mathbf{N}'\mathbf{P} + \dots \\
&\qquad \dots + \mu_k\mathbf{M}'\left(\mathbf{s}_{i_k} - \mathbf{s}_{j_k}\right)\Delta_{q,k}^2(t)\left(\mathbf{s}_{i_k} - \mathbf{s}_{j_k}\right)'\mathbf{M}\Bigg],
\end{aligned}$$

where

$$\mathbf{C}_\epsilon := \frac{1}{2}\sum_{k=1}^{|\mathscr{E}|}\left[\left(\mathbf{s}_{i_k} - \mathbf{s}_{j_k}\right)Q_{i_k j_k}(1 + \cos(\epsilon_k))\left(\mathbf{s}_{i_k} - \mathbf{s}_{j_k}\right)'\right],$$

and $\forall k \in \{1, 2, \dots, |\mathscr{E}|\}$, $\mu_k > 0$ are additional scalar variables that help to numerically relax the conservatism introduced by using the bound (24). This expression cannot be evaluated as we assume that the uncertain quantities $\Delta_{p,k}(t) \in \mathbb{R}$ and $\Delta_{q,k}(t) \in \mathbb{R}$ are unknown. However, from the known uncertainty bounds (12) and (13), we have that

$$\Delta_{p,k}^2(t) \le \sin^2(\epsilon_k),$$
$$\Delta_{q,k}^2(t) \le \frac{(1 - \cos(\epsilon_k))^2}{4}.$$

With this, and defining for clarity,

$$\mathbf{R}_k := m_k\mathbf{M}'\left(\mathbf{s}_{i_k} - \mathbf{s}_{j_k}\right)\left(\mathbf{s}_{i_k} - \mathbf{s}_{j_k}\right)'\mathbf{M},$$
$$\mathbf{z}_k := \mathbf{N}\left(\mathbf{s}_{i_k} + \mathbf{s}_{j_k}\right)P_{i_k j_k}, \text{ and}$$
$$\mathbf{w}_k := \mathbf{N}\left(\mathbf{s}_{i_k} - \mathbf{s}_{j_k}\right)Q_{i_k j_k},$$

with

$$m_k := \sin^2(\epsilon_k) + \frac{(1-\cos(\epsilon_k))^2}{4} = \frac{1}{4}(1-\cos(\epsilon_k))(3\cos(\epsilon_k) + 5),$$

an upper bound for the term of stability condition (22) becomes

$$\begin{aligned}
&\mathbf{PN}(\nabla_{\boldsymbol{\delta}}\mathbf{c})\mathbf{M} + \mathbf{M}'(\nabla_{\boldsymbol{\delta}}\mathbf{c})'\mathbf{N}'\mathbf{P} \\
&\quad \le \mathbf{PNC}_\epsilon\mathbf{M} + \mathbf{M}'\mathbf{C}_\epsilon'\mathbf{N}'\mathbf{P} + \dots \\
&\quad \dots + \sum_{k=1}^{|\mathscr{E}|}\left[\frac{1}{\mu_k}\mathbf{P}\mathbf{z}_k\mathbf{z}_k'\mathbf{P} + \frac{1}{\mu_k}\mathbf{P}\mathbf{w}_k\mathbf{w}_k'\mathbf{P} + \mu_k\mathbf{R}_k\right].
\end{aligned}$$

Making use of this upper bound for condition (22), we then find that a sufficient condition for stability is to impose negativity of the following expression:

$$\begin{aligned}
&\mathbf{PA} + \mathbf{A}'\mathbf{P} + \mathbf{PNC}_\epsilon\mathbf{M} + \mathbf{M}'\mathbf{C}_\epsilon'\mathbf{N}'\mathbf{P} \\
&\quad + \sum_{k=1}^{|\mathscr{E}|}\left[\mu_k\mathbf{R}_k + \frac{1}{\mu_k}\mathbf{P}\mathbf{z}_k\mathbf{z}_k'\mathbf{P} + \frac{1}{\mu_k}\mathbf{P}\mathbf{w}_k\mathbf{w}_k'\mathbf{P}\right] < 0.
\end{aligned}$$

This expression is not linear with respect to its variables because of the terms including multiplication of $\mathbf{P} > 0$ and $\mu_k > 0$. This can be solved by using Schur's complement to obtain the following Linear Matrix Inequality (LMI):

$$\begin{bmatrix}
\mathscr{M}_{11} & \text{row}\{\mathbf{P}\mathbf{z}_k\}_{k=1}^{|\mathscr{E}|} & \text{row}\{\mathbf{P}\mathbf{w}_k\}_{k=1}^{|\mathscr{E}|} \\
\star & -\text{diag}\{\mu_k\}_{k=1}^{|\mathscr{E}|} & \mathbf{0} \\
\star & \star & -\text{diag}\{\mu_k\}_{k=1}^{|\mathscr{E}|}
\end{bmatrix} < 0, \tag{25}$$

where

$$\mathscr{M}_{11} := \mathbf{PA} + \mathbf{A}'\mathbf{P} + \mathbf{PNC}_\epsilon\mathbf{M} + \mathbf{M}'\mathbf{C}_\epsilon'\mathbf{N}'\mathbf{P} + \sum_{k=1}^{|\mathscr{E}|}\mu_k\mathbf{R}_k.$$

With help of any standard LMI software as SeDuMi [34] parsed by YALMIP [15], by replacing matrices **A**, **M**, and **N** adequately, (25) can be used to verify either power sharing or synchronization of the microgrid in a neighborhood of the operation point $\boldsymbol{\theta} = \mathbf{0}$ by treating the non-linearities of the model as parameter uncertainties. A procedure to estimate the region of attraction of the operation point can also be developed from this expression.

### 4.5. Affine model validation

The difference between the affine and the non-linear model of the grid becomes relevant when the magnitude of the angle differences is large and the assumption $\boldsymbol{\theta} \approx \mathbf{0}$ does not hold. Therefore, a procedure to corroborate or to discard the affine model as a valid analysis tool needs to be consider. To do this, we can estimate the value of the angle differences vector $\boldsymbol{\theta}$ from the linear model, and then validate this estimation by comparing the measured generated power with the prediction of the nonlinear model using the estimated differences vector.

If we assume that the vectors $\mathbf{y} \in \mathbb{R}^N$ and $\mathbf{d} \in \mathbb{R}^N$ are known, through the affine approximation of the grid we have that

$$\begin{aligned}
\mathbf{y} \approx \mathbf{C}\boldsymbol{\delta} + \mathbf{d} &\Rightarrow \mathbf{C}^+(\mathbf{y} - \mathbf{d}) \approx \mathbf{C}^+\mathbf{C}\boldsymbol{\delta} \\
&\Rightarrow \mathbf{C}^+(\mathbf{y} - \mathbf{d}) \approx (\mathbf{I} - \mathbf{J})\boldsymbol{\delta} \\
&\Rightarrow \mathbf{D}\mathbf{C}^+(\mathbf{y} - \mathbf{d}) \approx \mathbf{D}(\mathbf{I} - \mathbf{J})\boldsymbol{\delta} \\
&\Rightarrow \mathbf{D}\mathbf{C}^+(\mathbf{y} - \mathbf{d}) \approx \mathbf{D}\boldsymbol{\delta} \\
&\Rightarrow \mathbf{D}\mathbf{C}^+(\mathbf{y} - \mathbf{d}) \approx \boldsymbol{\theta}.
\end{aligned}$$

Therefore, an approximation of the angle differences between neighboring nodes can be easily obtained by calculating $\hat{\boldsymbol{\theta}} := \mathbf{D}\mathbf{C}^+(\mathbf{y} - \mathbf{d}) \approx \boldsymbol{\theta}$.

To verify that this approximation is accurate enough, a non linear open-loop observer can be defined as

$$\hat{\mathbf{y}} = \mathbf{c}(\hat{\boldsymbol{\theta}}) + \mathbf{d}.$$

The error between the measurement injected power $\mathbf{y}$ and the estimated injected power $\hat{\mathbf{y}}$ can be defined. The norm of this quantity, $\|\mathbf{y} - \hat{\mathbf{y}}\|$, is an indicator of how good the approximation of the angle differences through the vector $\hat{\boldsymbol{\theta}}$ is.

## 5. Numeric example

### 5.1. Microgrid description and simulation

Consider the microgrid depicted in Fig. 4 with $N = 4$ generation units. The nominal parameters of the lines and loads are given in Table 1. The load parameters are only an estimation of the nominal value and change with time. The nominal parameters of the generation units are shown in Table 2. All simulations are performed by implementing the microgrid circuit and model of the generation units with help of the software PLECS© Plexim, v.4.0.3.

For simulation porpoises we are going to consider that the load behaves as depicted in Fig. 5, maintaining during the first 20 s the nominal values before individually changing at 20, 25, 30, and 35 s. For arbitrary initial conditions, during the first 5 s of simulation

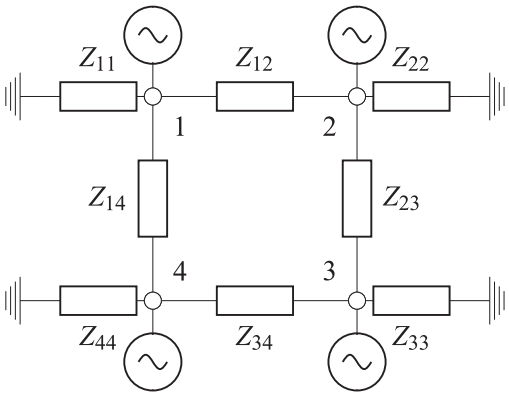


**Fig. 4.** Circuital description of the example microgrid.

**Table 1**
Line and load nominal parameters.

| | i | j | $R_{ij}[\Omega]$ | $L_{ij}[mH]$ |
|---|---|---|---|---|
| Lines | 1 | 2 | 0.630 | 1.2900 |
| | 2 | 3 | 0.140 | 0.2540 |
| | 3 | 4 | 0.580 | 1.3400 |
| | 1 | 4 | 0.128 | 0.1324 |
| Loads | 1 | 1 | 182.0042 | 190.4189 |
| | 2 | 2 | 82.6027 | 76.6886 |
| | 3 | 3 | 203.3016 | 162.1858 |
| | 4 | 4 | 166.0120 | 107.3028 |

we consider that no control action is performed. That is $\forall t < 5$, $\mathbf{L} = \mathbf{0}$ and $\mathbf{K} = \mathbf{0}$. During the following 5 s only a primary controller strategy is considered with, $\forall t \geq 5$,

**Table 2**
Generation units nominal parameters.

| $i$ | $S_i = \chi_i$[kVA] | $V_{RMS}$[V] | $f$[Hz] | $\kappa$ |
|---|---|---|---|---|
| 1 | 1.60 | 220 | 50 | 0.01 |
| 2 | 1.60 | | | |
| 3 | 0.80 | | | |
| 4 | 0.80 | | | |

$$\mathbf{L} = -1\mathbf{I} - \hat{L}(\mathcal{G}_w) = -\begin{bmatrix} 4 & -1 & -1 & -1 \\ -1 & 4 & -1 & -1 \\ -1 & -1 & 4 & -1 \\ -1 & -1 & -1 & 4 \end{bmatrix},$$

and $\mathbf{K} = \mathbf{0}$. For $t \geq 10$, the secondary action of the controller is changed to

$$\mathbf{K} = -\mathbf{1}\mathbf{k}' = -k\mathbf{1}\mathbf{s}_4' = -0.3501\begin{bmatrix} 0 & 0 & 0 & 1 \\ 0 & 0 & 0 & 1 \\ 0 & 0 & 0 & 1 \\ 0 & 0 & 0 & 1 \end{bmatrix}$$

and maintained like this for the rest of the simulation time. Under these simulation conditions, Fig. 6 shows the development of the interest variables. It is clear that the microgrid reaches both objectives when both control actions are different from zero (for times greater than 10 s), even after abrupt changes of the load. Coherently, $\forall t \geq 10$, matrices $\mathbf{G}_y := \kappa\mathbf{TFCLT}^+$ and $\mathbf{G}_K := \kappa\mathbf{LFC} + \mathbf{K}$ are Hurwitz.

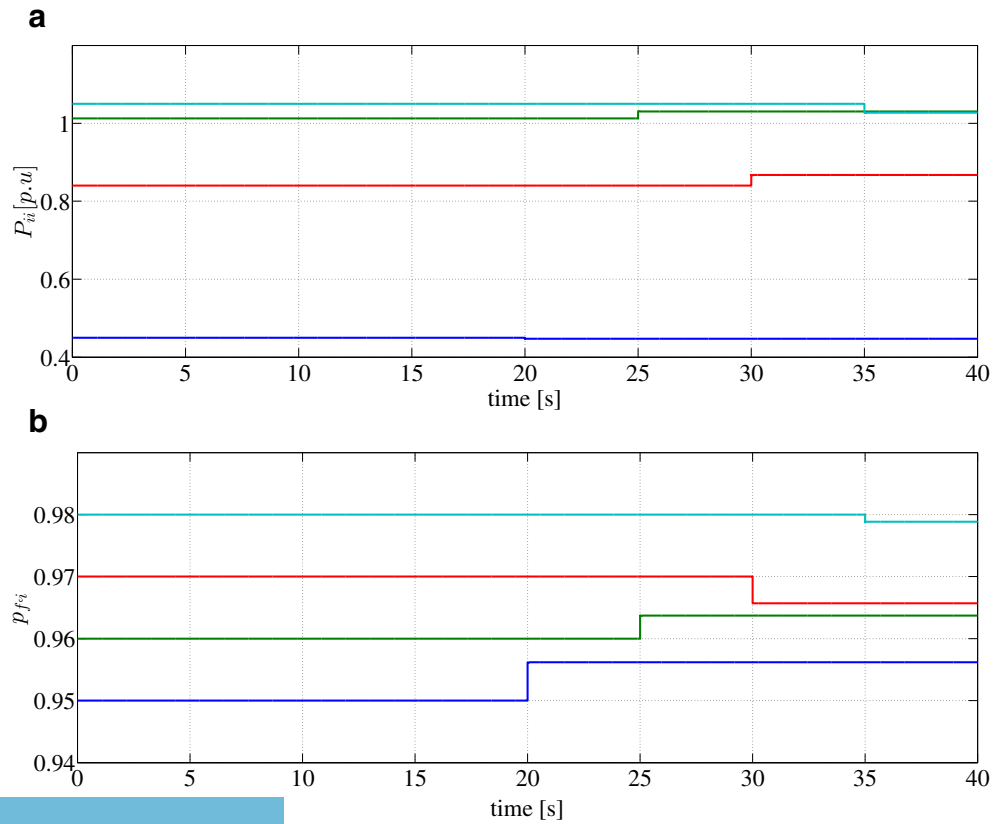


**Fig. 5.** Load behavior in Examples. a) Per unit load active power $\tilde{P}_{ii}[p.u.]$, and b) Power factor $p_{f,i} := \cos(\arctan(\omega_{o,i}L_{ii}/R_{ii}))$, at node 1:—, node 2:—, node 3:—, node 4:—.

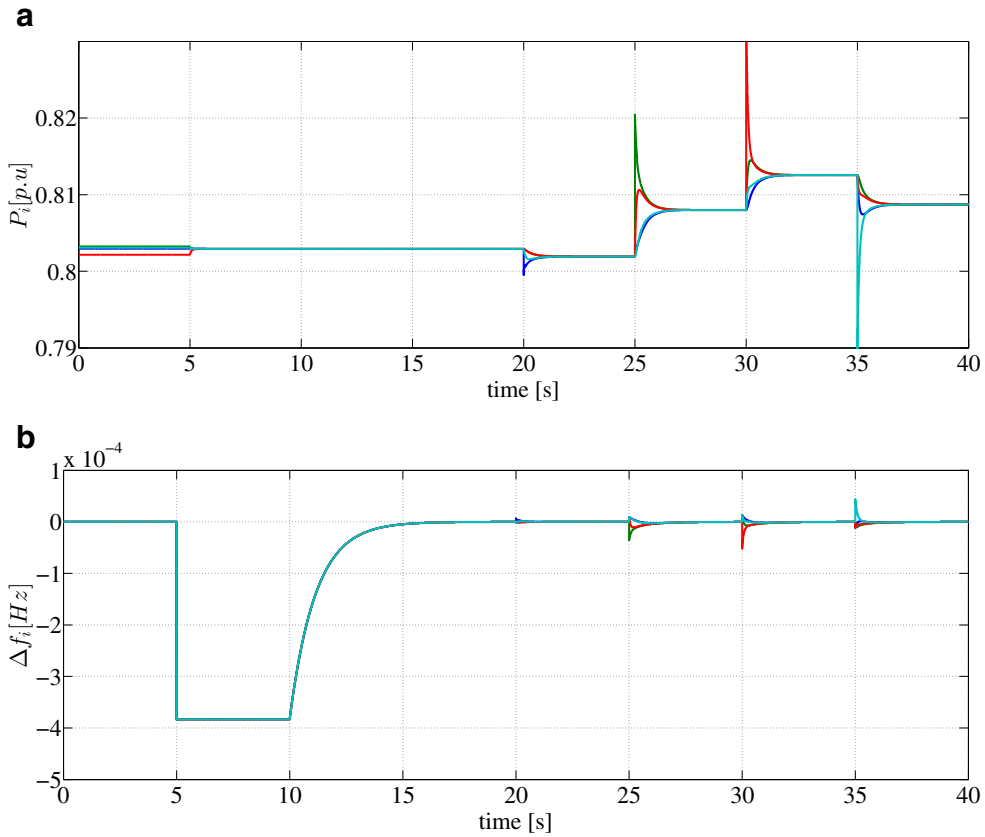


**Fig. 6.** Behavior of the grid without control for $t \leq 5$, with only primary droop-Laplacian controller $\mathbf{L} = -\mathbf{I} - \hat{L}(\mathscr{G}_w)$ for $t \in [5, 10]$, and with primary droop-Laplacian controller and distributed secondary controller $\mathbf{K} = -k\mathbf{1}\mathbf{s}_4'$ for $t \geq 10$. a) Per unit generated active power $\tilde{P}_i[p.u.]$, and b) Frequency deviation at each inverter $\Delta f_i := (u^{\Psi_i} - \omega)/(2\pi)[Hz]$.

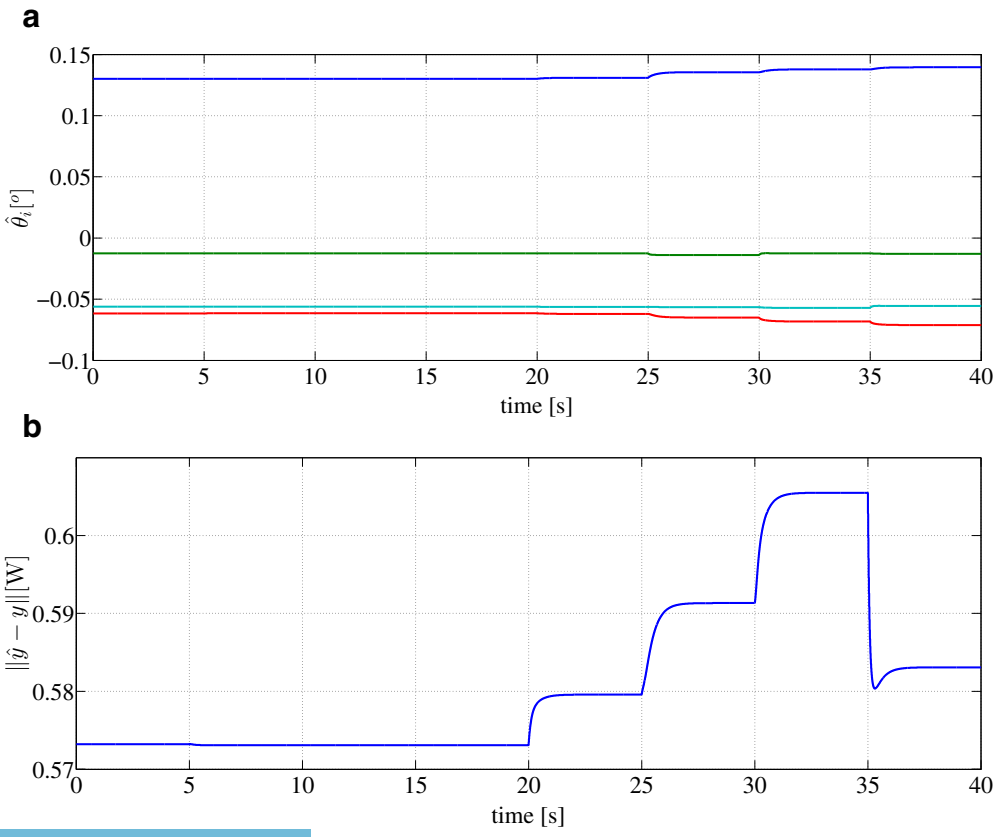


**Fig. 7.** Behavior of the grid without control for $t \leq 5$, with only primary droop-Laplacian controller $\mathbf{L} = -\mathbf{I} - \hat{L}(\mathscr{G}_w)$ for $t \in [5, 10]$, and with primary droop-Laplacian controller and distributed secondary controller $\mathbf{K} = -k\mathbf{1}\mathbf{s}_4'$ for $t \geq 10$. a) Approximated angle differences $\hat{\boldsymbol{\theta}}_i[^\circ]$, and b) Error between estimated and measured output $\|\hat{\mathbf{y}} - \mathbf{y}\|[W]$.

### 5.2. Affine model validation

The angle differences vector can be define as $\boldsymbol{\theta} = \mathbf{D}\boldsymbol{\delta}$ with the following matrix:

$$\mathbf{D} = \begin{bmatrix} 1 & -1 & 0 & 0 \\ 0 & 1 & -1 & 0 \\ 0 & 0 & 1 & -1 \\ -1 & 0 & 0 & 1 \end{bmatrix}.$$

Each element of $\boldsymbol{\theta}$ is associated to one of the four grid lines. Using the control strategy defined in the previous section, i.e., $\mathbf{L} = -\mathbf{I} - \hat{L}(\mathscr{G})$ and $\mathbf{K} = -k\mathbf{1}\mathbf{s}_4'$, LMI (25) is feasible for the power sharing and the synchronization cases when $\forall k \in \{1, 2, 3, 4\}$, $\epsilon_k = \epsilon = 20^\circ$. Naturally, it also holds for smaller values of $\epsilon > 0$. That is, we know that at least for angle differences smaller than 20°, the grid will reach power sharing and synchronization to nominal frequency.

This stability test could be considered conservative because of the chosen approximation and the higher bounds imposed to the Lyapunov condition. Nevertheless, this is not an issue when the microgrid is operated around the point $\theta \approx \mathbf{0}$. Indeed, note that under the same simulation conditions as before, the approximation $\hat{\boldsymbol{\theta}} = \mathbf{D}\mathbf{C}^{+}(\mathbf{y} - \mathbf{d})$ of the angle differences is depicted in Fig. 7 a). Observe that the angle differences are in absolute value smaller than 0.15°, considerably smaller than the theoretical border of 20° obtained with help of LMI (25).

In Fig. 7 b), the norm of the error between the measured injected power, $\mathbf{y}$, and the non linear open loop estimation $\hat{\mathbf{y}} = \mathbf{c}(\hat{\boldsymbol{\theta}}) + \mathbf{d}$ is shown. Note that this value is less than $0.65[W]$ in a context where the power is measured in $[kW]$. This represents less than 0.03% of error with respect to the total generated power. From here we can conclude that the approximation of the grid by a linear model is accurate enough for analysis porpoises.

## 6. Conclusion

In this paper we have dealt simultaneously with the problems of frequency synchronization and active power sharing in three-phase VSI interfaced microgrids. This is an example of a network of agents that search consensus but are connected by hardware nonlinear relationships. By distinguishing between the process plant, the control objectives, and the feedback controller, we are entitled to study the behavior of the closed loop system with respect to the control objectives in a systematic way considering the nonlinear model of the power flux through the grid. We show that it is possible to study power sharing and synchronization by defining a robust approximation of the non-linearities. We further suggest an LMI based methodology to verify that a given control strategy makes the microgrid reach the control objectives and a procedure to verify if the robust approximation is accurate enough for analysis. Future work includes the use of more complex models for the agents, that might consider clock drifts or harmonic components, lines faults and parameters uncertainty, and comparison with other control strategies in an experimental setup.

## Acknowledgment

This work is partially funded by the Chilean National Agency of Technology and Scientific Research (CONICYT), Grant no. 7213005.

## Supplementary material

Supplementary material associated with this article can be found, in the online version, at doi:10.1016/j.ejcon.2018.05.001.

## References

[1] A. Abdessameud, A. Tayebi, On consensus algorithms design for double integrator dynamics, Automatica 49 (2013) 253–260.
[2] P.M. Anderson, A.A. Fouad, Power System Control and Stability, 2nd edition, IEEE Press, 2003.
[3] A. Ben-Israel, T.N.E. Greville, Generalized Inverses. Theory and Applications, 2nd edition, Springer, 2003.
[4] A. Bidram, F.L. Lewis, A. Davoudi, Distributed control systems for small-scale power networks, IEEE Control Syst. Mag. (2014) 56–77.
[5] Y. Cao, W. Yu, W. Ren, G. Chen, An overview of recent progress in the study of distributed multi-agent coordination, IEEE Tran. Ind. Inform. 9 (2012) 427–438.
[6] F. Dörfler, F. Bullo, Kron reduction of graphs with applications to electrical networks, IEEE Trans. Circuits Syst. 60 (2013).
[7] C. Godsil, G. Royle, Algebraic Graph Theory, Springer-Verlag, 2001.
[8] D. Goldin, S.A. Attia, J. Raisch, Consensus for double integrator dynamics in heterogeneous networks, in: Proceedings of 49th IEEE Conference on Decision and Control (CDC), 2010.
[9] D. Goldin, J. Raisch, Controllability of second order leader-follower systems, in: Proceedings of Second IFAC Workshop on Estimation and Control of Networked Systems, 2010.
[10] J.M. Guerrero, M. Chandorkar, T.-L. Lee, P.C. Loh, Advanced control architectures for intelligent microgrids, part I, IEEE Trans. Ind. Electron. 60 (2013) 1254–1262.
[11] F. Guo, C. Wen, J. Mao, Y.-D. Song, Distributed secondary voltage and frequency restoration control of droop-controlled inverter-based microgrids, IEEE Trans. Ind. Electron. 62 (2015).
[12] P. Kundur, Power System Stability and Control, McGraw-Hill, 1994.
[13] Z. Li, W. Ren, X. Liu, L. Xie, Distributed consensus of linear multi-agent systems with adaptive dynamic protocols, Automatica 49 (2013) 1986–1995.
[14] K.D. Listmann, J. Adamy, L. Scardovi, Synchronisierung indentischer linearer systeme - ein zugang über LMIs, Automatisierungstechnik 59 (2011) 563–573.
[15] J. Löfberg, YALMIP: a toolbox for modeling and optimization in MATLAB, in: Proceedings of 2004 IEEE International Symposium on Computer Aided Control Systems Design, 2004, pp. 284–289.
[16] M. Mesbahi, M. Egerstedt, Graph Theoretic Methods in Multiagent Networks, Princeton University Press, 2010.
[17] R. Olfati-Saber, J.A. Fax, R.M. Murray, Consensus and cooperation in networked multi-agent systems, in: Proceedings of the IEEE, 95, 2007.
[18] M. Parada Contzen, Consensus in networks with arbitrary time invariant linear agents, Eur. J. Control 38 (2017) 52–62.
[19] M. Parada Contzen, J. Raisch, Active power consensus in microgrids, in: Proceedings of International Symposium on Smart Electric Distribution Systems and Technologies (EDST), 2015.
[20] M. Parada Contzen, J. Raisch, Reactive power consensus in microgrids, in: Proceedings of European Control Conference (ECC) 2016, 2016.
[21] J.A. Peças Lopes, C.L. Moreira, A.G. Madureira, Defining control strategies for microgrids islanded operation, IEEE Trans. Power Syst. 21 (2006).
[22] N. Pogaku, M. Prodanović, T.C. Green, Modeling, analysis and testing of autonomous operation of an inverter-based microgrid, IEEE Trans. Power Electron. 22 (2007) 613–625.
[23] W. Ren, R.W. Beard, Distributed Consensus in Multi-vehicle Cooperative Control, Springer, 2010.
[24] W. Ren, Y. Cao, Distributed coordination of multi-agent networks, Communications and Control Engineering Series, Springer-Verlag, 2011.
[25] J. Rocabert, Á. Luna, F. Blaabjerg, P. Rodríguez, Control of power converters in AC microgrids, IEEE Trans. Power Electron. 27 (2012).
[26] L. Scardovi, R. Sepulchre, Synchronization in networks of identical linear systems, Automatica 45 (2009) 2557–2562.
[27] J. Schiffer, A. Anta, T.D. Trung, J. Raisch, T. Sezi, On power sharing and stability in autonomous inverter-based microgrids, in: Proceedings of the 51st IEEE Conference on Decision and Control, 2012.
[28] J. Schiffer, F. Dörfler, E. Fridman, Robustness of distributed averaging control in power systems: time delays & dynamic communication topology, Automatica 80 (2017) 261–271.
[29] J. Schiffer, D. Goldin, J. Raisch, T. Sezi, Synchronization of droop-controlled microgrids with distributed rotational and electronic generation, in: Proceedings of the 52nd IEEE CDC, 2013.
[30] J. Schiffer, T. Seel, J. Raisch, T. Sezi, A consensus-based distributed voltage control for reactive power sharing in microgrids, in: Proceedings of Thirteenth ECC, 2014.
[31] E. Semsar-Kazerooni, K. Khorasani, Optimal consensus seeking in a network of multiagent systems: an LMI approach, IEEE Trans. Syst. Man Cybern. 40 (2010) 540–547.
[32] J.W. Simpson-Porco, F. Dörfler, F. Bullo, Synchronization and power sharing for droop-controlled inverters in islanded microgrids, Automatica 49 (2013) 2603–2611.
[33] J.W. Simpson-Porco, Q. Shafiee, F. Dörfler, J.C. Vasquez, J.M. Guerrero, F. Bullo, Secondary frequency and voltage control of islanded microgrids via distributed averaging, IEEE Trans. Autom. Control 62 (2015) 7025–7038.
[34] J.F. Sturm, Using SeDuMi 1.02, a MATLAB toolbox for optimization over symmetric cones, Optim. Methods Softw. 11 (1999) 625–653.
[35] P. Wieland, R. Sepulchre, F. Allgöwer, An internal model principle is necessary and sufficient for linear output synchronization, Automatica 47 (2011) 1068–1074.
[36] D. Zhang, X. Wang, L. Meng, Consensus problems for high-order LTI systems: a decentralized static output feedback method, Int. J. Innov. Comput. Inf. Control 9 (2013) 2143–2154.